

Context-specific control over the neural dynamics of temporal attention by the human cerebellum

Assaf Breska* and Richard B. Ivry

Physiological methods have identified a number of signatures of temporal prediction, a core component of attention. While the underlying neural dynamics have been linked to activity within cortico-striatal networks, recent work has shown that the behavioral benefits of temporal prediction rely on the cerebellum. Here, we examine the involvement of the human cerebellum in the generation and/or temporal adjustment of anticipatory neural dynamics, measuring scalp electroencephalography in individuals with cerebellar degeneration. When the temporal prediction relied on an interval representation, duration-dependent adjustments were impaired in the cerebellar group compared to matched controls. This impairment was evident in ramping activity, beta-band power, and phase locking of delta-band activity. These same neural adjustments were preserved when the prediction relied on a rhythmic stream. Thus, the cerebellum has a context-specific causal role in the adjustment of anticipatory neural dynamics of temporal prediction, providing the requisite modulation to optimize behavior.

Copyright © 2020
The Authors, some
rights reserved;
exclusive licensee
American Association
for the Advancement
of Science. No claim to
original U.S. Government
Works. Distributed
under a Creative
Commons Attribution
NonCommercial
License 4.0 (CC BY-NC).

INTRODUCTION

Temporal anticipation is essential for survival in our dynamic world. Whether playing sports, listening to music, or driving, our brain is able to use temporal regularities to predict the timing of upcoming events (1, 2). These predictions guide proactive allocation of attentional resources and preparation of adaptive responses, expressed in various contexts by the behavioral benefits observed when predictions are confirmed and costs when violated (3–10). Neurophysiological recordings in humans and nonhuman primates (NHPs) have associated temporal prediction and attention with a set of neural signatures reflecting activity in cortico-striatal networks (1). First, ramping neuronal activity, expressed in human scalp recordings as the contingent negative variation (CNV) potential, is adjusted such that it peaks near the expected time of an upcoming event (6–8, 11–14). Second, the power of movement-related beta-band activity decreases just before the expected time of the imperative (7, 15–20). Third, an increase in phase consistency of low-frequency activity (e.g., delta range, 0.5 to 3 Hz) is observed across repeated instances of the same interval in temporally predictable contexts, putatively reflecting alignment of high excitability states at an expected time (3, 4, 6, 21, 22). These patterns are evident in NHP recordings in frontal, parietal, and basal ganglia circuits, regions that feature prominently in human functional magnetic resonance imaging (fMRI) studies of temporal anticipation (9, 23–27).

However, a strict cortico-striatal view of temporal anticipation was recently challenged by evidence that individuals with cerebellar degeneration (CD) failed to exhibit behavioral benefits from temporal cues on a simple detection task (28). The impairment was limited to conditions in which temporal anticipation was based on associations between cues and isolated intervals (6, 8–10), but not when based on a periodic signal (3–7). These findings established a context-specific role of the human cerebellum in temporal anticipation, extending prior work that had emphasized the critical role of the cerebellum in tasks that require explicit timing (29–34).

Given that temporal anticipation involves neural dynamics within a cortico-striatal network, a fundamental question concerns how a cerebellar timing system might interact with this network. Electrophysiological recordings in NHPs have shown beta-band activity and ramping activity in the cerebellum during timed movements (35–38), and neuroimaging studies have reported increased cerebellar activation and cerebro-cerebellar correlation during temporal anticipation (39, 40). Moreover, an increase in the cerebellar blood oxygen level-dependent response is observed during the buildup of the CNV, paralleling activity in premotor areas (41). However, given the correlational nature of fMRI and its low temporal resolution, it is not clear whether cerebellar activity provides a modulatory input to cortico-striatal circuits involved in temporal prediction, reflects cortico-striatal activity projected to the cerebellum, or affects temporal preparation independently of cortico-striatal activity (e.g., by modulating descending motor pathways).

Aiming to identify the causal role (if any) of the cerebellum in the cortical dynamics of temporal anticipation, we measured electroencephalography (EEG) in individuals with CD while they performed two temporal prediction tasks. In one task, prediction was based on an interval representation; in the other, the prediction was derived from a rhythmic stream. On the basis of our previous study (28), we expected to find a behavioral impairment in the CD group for interval-based, but not rhythm-based prediction. Our primary goal was to examine the role of the cerebellum in the CNV, delta-band phase locking, and beta-band amplitude. For each of these neural patterns, we considered three models with respect to the expected deficits in the Interval task (Fig. 1A). First, the cerebellum may be critical for the generation of extracerebellar (e.g., cortico-striatal) ramping, delta-band, and/or beta-band activity. By this “cerebellar generation” model, these patterns would be abolished or severely attenuated in the CD group. Second, the cerebellum may be critical for the temporal adjustment, rather than generation, of these neural patterns. By this “cerebellar adjustment” model, the CD group would still demonstrate these neural patterns before anticipated events, but no duration-dependent adjustments would be observed in the CNV and beta suppression, and delta phase-locking would not increase to a similar extent as in controls. Third, the cortico-striatal mechanisms reflected in these patterns may operate

Department of Psychology and Helen Wills Neuroscience Institute, University of California, Berkeley, 2121 Berkeley Way, Berkeley, CA 94720, USA.

*Corresponding author. Email: assaf.breska@berkeley.edu

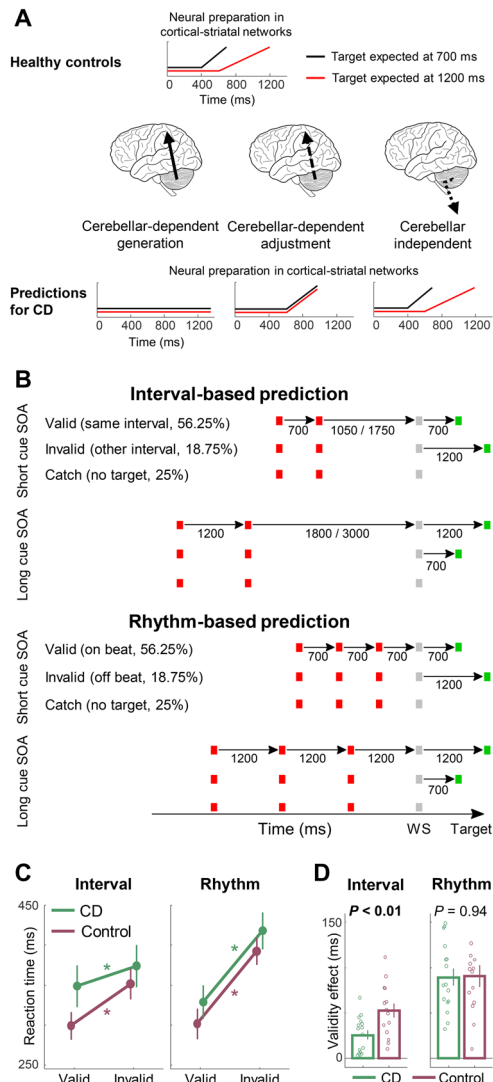


Fig. 1. Paradigm and behavioral results. (A) Top: Controls are expected to show adjustment in cortico-striatal anticipatory neural activity as a function of the cue-to-target interval. Bottom: Three hypotheses and their associated predictions concerning the role of cerebellum in modulating cortico-striatal attentional networks following interval-based temporal cues. Left: Cerebellar-dependent generation hypothesis of neural preparation predicts no neural preparation in the CD group. Middle: Cerebellar-dependent adjustment hypothesis predicts neural preparation that is not adjusted by knowledge of the expected interval (for illustration purposes, anticipatory activity is depicted as peaking at the average interval of 950 ms regardless of the expected target time). Right: Cerebellar-independent hypothesis predicts a similar pattern to controls. (B) Experimental paradigm. Participants viewed a stream of flickering colored squares and provided a speeded response upon detecting a target (green square). Top: Interval task. Two red squares were separated by either a short or a long stimulus onset asynchrony (SOA). After a variable delay period, a warning signal (white square) appeared, preceding the target. The interval between the warning signal and target could be the same SOA (valid) or the other SOA (invalid). Bottom: Rhythm task. Three red squares and a warning signal appeared with identical SOA (short/long). Valid and invalid trials were as in the Interval task. In both tasks, short SOA = 700 ms, long SOA = 1200 ms. On 25% of the trials, no target was presented (catch trials), and participants were to withhold response. (C) Behavioral results. Mean reaction times (RTs) for the CD and control groups for the Interval and Rhythm tasks. Error bars represent 1 SEM. *P < 0.05. (D) Magnitude of validity effect (Invalid – Valid). The validity effect is smaller in the CD group in the Interval task but has a similar magnitude in the Rhythm task. Error bars represent 1 SEM.

independently of the cerebellum. By this “cerebellar independent” model, EEG patterns in the CD group would be similar to those observed in control participants.

A second goal of the study was to examine how an impairment in interval-based prediction might affect EEG signatures of temporal anticipation under rhythm-based prediction. This question is relevant to the current debate in the literature regarding the context specificity of these neural signatures of temporal prediction (42–46). Increased delta-band phase locking has been interpreted as reflecting rhythm-specific prediction mechanisms, such as the entrainment of endogenous oscillations (3, 4, 21). However, similar neural adjustments are observed for aperiodic streams that enable interval-based prediction (6). This has motivated the hypothesis that neural patterns observed during rhythmic predictions may be mediated by the repeated operation of an interval-based mechanism given that a periodic stream consists of a series of concatenated intervals (47). Alternatively, a similar neural adjustment in rhythm- and interval-based contexts may result from a shared downstream process that is driven by distinct, context-specific mechanisms. Finding a selective disruption in the Interval task would be consistent with the latter hypothesis, in this case pointing to the necessity of the cerebellum for interval-based adjustment. However, finding that some signatures of neural anticipation are disrupted in both tasks in the CD group would indicate that they are driven by cerebellar-dependent interval-based mechanism, even in rhythmic contexts.

RESULTS

Individuals with CD ($n = 16$) and controls ($n = 14$) completed two variants of a temporal prediction task in the visual modality (Fig. 1B) (6, 28). The participants performed a detection task, making a button press as quickly as possible in response to a target that was preceded by a warning signal. In turn, the warning signal was preceded by a cue that indicated the likely interval between the warning signal onset and target onset [stimulus onset asynchrony (SOA)]. In the Interval task, the cue consisted of two stimuli whose SOA was either 700 or 1200 ms. The warning signal appeared after an interval of either 1.5 or 2.5 times the cue SOA, making the stimulus stream non-isochronous. In the Rhythm task, the temporal cue was defined by a periodic stream of four stimuli, with the last stimulus being the warning signal. The stimuli were separated by a fixed SOA of 700 or 1200 ms. In both tasks, the SOA between the warning signal and target matched the cue SOA on 75% of the trials (valid trials); on 25%, the interval between the warning signal and the target matched the other, uncued SOA (invalid trials). We also included catch trials in which no target appeared, to discourage premature responses (10). We predicted that the CD group will exhibit a behavioral impairment in the Interval but not Rhythm task and hypothesized that this impairment would be accompanied by abnormalities in some or all of the EEG signatures of temporal anticipation. Therefore, for each behavioral and neural measure, the analyses were designed to test the temporal anticipation effect within each group and compare the two groups within each task.

Reduced behavioral benefits of interval-based, but not rhythm-based, temporal prediction in CD

In our design, temporal anticipation should lead to faster reaction times (RTs) on cue-valid trials compared to cue-invalid trials (we refer to this as “validity effect”) (5, 8, 9). This was indeed found in

our data across all conditions and groups [omnibus mixed analysis of variance (ANOVA), $F(1,28) = 138.2, P = 3 \times 10^{-12}, \eta_p^2 = 0.83$]. However, the magnitude of the effect varied between groups and tasks [Task \times Group \times Validity interaction, $F(1,28) = 4.4, P = 0.02, \eta_p^2 = 0.14$]. We next turned to the critical question of whether the CD group was impaired relative to controls, using planned contrasts comparing the groups within each task. In the interval task (Fig. 1, C and D, left panels), the validity effect was smaller in the CD relative to the control group [25 and 53 ms for the CD and control groups, respectively; mixed ANOVA, Validity \times Group interaction: $F(1,28) = 8.75, P = 0.006, \eta_p^2 = 0.24$]. The within-group analyses using planned contrasts indicated that the validity effect was significant within each group [repeated-measures ANOVA, Control: $F(1,13) = 43.7, P = 1 \times 10^{-5}, \eta_p^2 = 0.77$; CD: $F(1,15) = 25.9, P = 1 \times 10^{-4}, \eta_p^2 = 0.63$].

Turning to the Rhythm task (Fig. 1, C and D, right panels), we found that the magnitude of the validity effect did not differ significantly between groups [CD, 89 ms; Control, 91 ms; interaction $F(1,28) = 0.01, P = 0.94, \eta_p^2 < 0.01$; Bayes factor, $BF_{10} = 0.34$, weak evidence in favor of the null hypothesis], with the validity effect again significant within both groups [Control, $F(1,13) = 54.9, P = 3 \times 10^{-6}, \eta_p^2 = 0.81$; CD, $F(1,15) = 89, P = 1 \times 10^{-7}, \eta_p^2 = 0.86$]. Direct comparison of the two tasks within each group revealed that the validity effect was larger in the Rhythm task in both groups [Validity \times Task interaction, Controls, $F(1,13) = 19, P = 8 \times 10^{-4}, \eta_p^2 = 0.59$; CD, $F(1,15) = 54.9, P = 2 \times 10^{-6}, \eta_p^2 = 0.79$].

In sum, participants were faster to detect a target that appeared at a cued point in time, compared to when the target appeared at an unexpected time. However, the CD group exhibited a reduced validity effect for interval-based predictions, but a normal validity effect for rhythm-based predictions.

CD abolishes temporal adjustment of CNV buildup in interval-based prediction

Temporal anticipation leads to adjustment of anticipatory ramping neural activity according to the expected interval, such that it peaks just before the expected time (11–14). In human EEG, this is expressed in the CNV, a negative potential typically elicited following a warning signal (6–8). To test the role of the cerebellum in this adjustment, we analyzed the CNV amplitude in a time window just before the early target time, where the difference between expecting the target at the early and late times should be maximal. We also used a cluster-based permutation analysis (48) without restriction to a specific time range. Temporal anticipation should lead to a more negative CNV amplitude following the short SOA cue compared to the long SOA cue, or what we will refer to as the “cue effect.”

Across all conditions, the CNV was observed after the warning signal with a typical fronto-central scalp distribution (Fig. 2A). Both groups showed a CNV buildup, expressed as a significant difference from baseline, following both cue durations in both tasks (all t 's > 2.65 , all P 's < 0.05 , all Cohen's $d > 0.7$; Fig. 2, B and C). Across groups and tasks, the CNV amplitude showed a cue effect [mixed ANOVA in predefined window: $F(1,28) = 19.9, P = 2 \times 10^{-4}, \eta_p^2 = 0.42$], although the magnitude of this effect varied as a function of Group and Task [Cue SOA \times Group \times Task: $F(1,28) = 2.94, P = 0.048, \eta_p^2 = 0.14$]. Planned contrasts within tasks revealed that in the Interval task, the cue effect was smaller in the CD group [Cue SOA \times Group interaction: $F(1,28) = 4.33, P = 0.046, \eta_p^2 = 0.13$; Fig. 2B]. Analysis of the Interval task within each group found a cue effect in controls [predefined time window: $t(13) = -3.12, P = 0.008$, Cohen's $d = 0.83$;

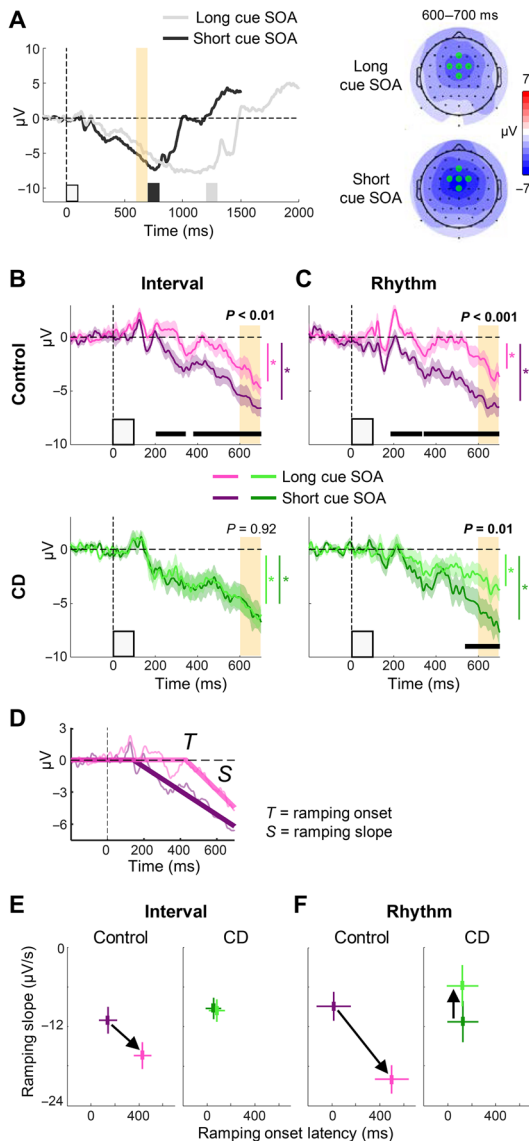


Fig. 2. CNV adjustment depends on the cerebellum in interval-based but not rhythm-based prediction. (A) CNV elicited following warning signal onset (0 ms) for the short and long cue SOA conditions, averaged across groups and tasks. Black and gray squares indicate expected target times. Scalp distribution depicted for a time window preceding the short SOA target (yellow bar). Green dots: predefined fronto-central electrode cluster used for the CNV analysis. (B) CNV in the Interval task following short SOA cue (dark color) or long SOA cue (light color). The cue effect observed in the control group (top) is abolished in the CD group (bottom). Yellow bars: Predefined window for analysis of CNV amplitude. Horizontal bars: Clusters showing significant difference between conditions ($P < 0.05$). Error margins indicate 1 SEM of the difference between expected SOAs. * $P < 0.05$ against baseline. (C) Same as (B) for the Rhythm task. A cue effect is observed in both groups. (D) Ramping activity model of the CNV buildup, allowing variation of ramping onset time (T) and ramping slope (S). The depicted model fit is for the control data in the Interval task. (E) Parameter estimates of the ramping model in the Interval task. The black arrow illustrates transition from short to long cue SOA. Controls show delayed ramping onset and steeper slope in the long SOA condition. The CD group shows no cue effect in either parameter. Horizontal and vertical error bars indicate 1 SEM of the difference between expected SOAs for ramping onset latency and slope, respectively. (F) Same as (E) for the Rhythm task. Controls show a similar pattern to the Interval task, whereas the CD group shows a cue effect in the slope parameter only, with a steeper slope in the short SOA condition, opposite that observed in the control group.

cluster-based permutation $P < 0.05$] but not in patients with CD [$t(15) = 0.1, P = 0.92, d = 0.03; \text{BF}_{10} = 0.26$, moderate evidence in favor of the null hypothesis; strongest cluster $P > 0.5$].

A different pattern was observed in the Rhythm task. Here, there was no difference in the cue effect between the two groups [$F(1,28) = 0.003, P = 0.96, \eta_p^2 < 0.01; \text{BF}_{10} = 0.33$, moderate evidence for the null hypothesis; Fig. 2C], with a cue effect observed in controls [$t(13) = -4.44, P = 7 \times 10^{-4}, d = 1.19$; cluster $P < 0.05$] and no Cue SOA \times Task interaction [$F(1,13) = 0.75, P = 0.4, \eta_p^2 = 0.05$]. The cue effect was also significant in the patients with CD [$t(15) = -2.96, P = 0.01, d = 0.74$; cluster $P < 0.05$], as was the interaction, with the cue effect larger in the Rhythm task [$F(1,15) = 6.78, P = 0.02, \eta_p^2 = 0.31$].

Thus, when temporal prediction relied on timing cued by an isolated interval, the CD group failed to exhibit temporal adjustment in the buildup of the CNV. In contrast, when temporal predictions relied on a rhythm, the CD group showed an adjustment of the CNV buildup, leading to similar difference in CNV amplitude before the early target SOA as in controls.

CNV modulation in the Rhythm task for the CD group is manifest as a change in slope rather than latency adjustment

Given that the CNV is reflective of ramping activity, its shape can be informative concerning the dynamics of preparatory resource allocation. Adjustment of ramping activity in response to different temporal goals can involve modulation of either its onset latency or its slope, as evident in NHP neural recordings (12, 37, 38, 49). To examine the effect of temporal anticipation on these parameters, we fit the CNV waveform generated between the warning signal onset and the earliest possible target time (700 ms) with a two-parameter linear ramping model (Fig. 2D), one corresponding to the slope and the other corresponding to onset latency [(6, 7); see validation in Materials and Methods]. Four fits were performed for each group (two tasks and two cue SOAs), with the data averaged across participants within a group. To compare the parameters between conditions, we used a permutation-based approach. For each comparison, we built a null distribution for the test statistic (e.g., latency when expecting short minus latency when expecting long) by shuffling the labels of exchangeable conditions for that comparison (50), re-averaging the shuffled data, fitting the model, and registering the randomized test statistic. A given comparison was considered statistically significant if the true test statistic exceeded 95% of the randomized test statistics.

For the latency parameter, CNV onset was earlier following the short cue SOA compared to the long cue SOA ($P < 0.05$). This effect differed between groups (Cue SOA \times Group interaction: $P < 0.05$), but the three-way interaction was not significant (Cue SOA \times Group \times Task, $P > 0.5$). Planned contrasts within each task found that the cue effect was smaller in the CD group in both tasks (Cue SOA \times Group interaction, both $P < 0.05$; Fig. 2, E and F). The control group showed a cue effect in both tasks (both P 's < 0.05 ; no difference in cue effect between tasks, Cue SOA \times Task interaction, $P > 0.05$). Notably, the CD group did not show a cue effect in either task (both P 's > 0.4 ; no difference in cue effect between tasks, $P > 0.5$). Thus, the absence of latency modulation in the CD group was evident for both interval-based and rhythm-based prediction.

For the slope parameter, the CNV slope was not significantly different following the short and long cue SOAs ($P > 0.05$). However, there was a three-way interaction (Cue SOA \times Group \times Task; $P < 0.05$). Planned contrasts revealed that in the Interval task, the

cue effect differed between the control and CD groups (Cue SOA \times Group interaction, both $P < 0.05$; Fig. 2E). In controls, the CNV slope was shallower following the short cue SOA compared to the long cue SOA ($P < 0.05$), while in the CD group, no cue effect was observed ($P > 0.5$). In the Rhythm task, the cue effect also differed between groups ($P < 0.05$; Fig. 2F). For the controls, the effect was in the same direction as in the Interval task ($P < 0.05$; no difference in cue effect between tasks, $P > 0.05$). In contrast, the CD group showed a steeper slope following the short cue SOA compared to the long cue SOA ($P < 0.05$). Moreover, the modulation of the slope was larger in the Rhythm task compared to the Interval task ($P < 0.05$). Thus, the adjustment of slope in the CD group was abolished for interval-based predictions and reversed for rhythm-based predictions.

CD reduces temporal alignment of low-frequency activity in interval-based but not rhythm-based prediction

Temporally predictive streams are associated with phase alignment of low-frequency activity during the anticipatory period, expressed as an increase in phase consistency across trials for a given expected target interval (3, 4, 6). To test the dependence of phase alignment on the cerebellum, we band-pass-filtered the EEG data to a delta-band frequency range that corresponds to the expected intervals (0.6 to 2 Hz, symmetrical around the frequencies corresponding to the expected intervals, see Materials and Methods) and calculated the inter-trial phase concentration (ITPC) index (51) following the warning signal (fig. S2). We used the same, predefined fronto-central electrode cluster as in the CNV analysis, allowing us to look at temporal consistency in signals associated with the systematic adjustments in the CNV (Fig. 3A, top) (an exploratory analysis revealed another cluster of increased ITPC in occipital electrodes, showing a similar pattern of results to that described below for the fronto-central cluster; fig. S3).

Across groups and tasks, ITPC increased before the early target window, with a frequency distribution that was centered on the delta range (Fig. 3A, bottom). Focusing on this range, we first examined the baseline epoch, when no temporal prediction was available, and found no difference in ITPC between the control and CD groups (between-subject permutation test: $P > 0.3$; Fig. 3, B and C, left). Across groups and tasks, delta ITPC before the early target was higher than baseline (permutation-based ANOVA, $P < 0.05$; Fig. 3B), but the magnitude of ITPC in this time window was different between groups and tasks (Group \times Task interaction, $P < 0.05$). Planned contrasts within each task revealed that in the Interval task, the ITPC increase was smaller in the CD group relative to controls (between-subject permutation test, $P < 0.05$; Fig. 3C, middle; see fig. S2 for single-subject data), though the ITPC increase relative to baseline was still significant in both groups (both P 's < 0.01). If ITPC in rhythm-based prediction reflects repeated interval-based mechanisms (6, 42–44), then it should be similarly reduced in the Rhythm task. However, the magnitude of ITPC increase in the Rhythm task did not differ between the two groups ($P > 0.8$; Fig. 3C, right), with both groups showing significant ITPC increase from baseline (Control: $P < 0.01$; CD: $P < 0.01$). The control group showed no difference in ITPC increase between tasks ($P > 0.8$), whereas for the CD group, the ITPC increase was larger in the Rhythm task ($P < 0.01$). Thus, the ITPC increase in rhythm-based prediction does not rely on cerebellar-dependent interval mechanisms.

The dissociation between the two tasks indicates that the ITPC increase in aperiodic contexts is mediated by a cerebellar-dependent

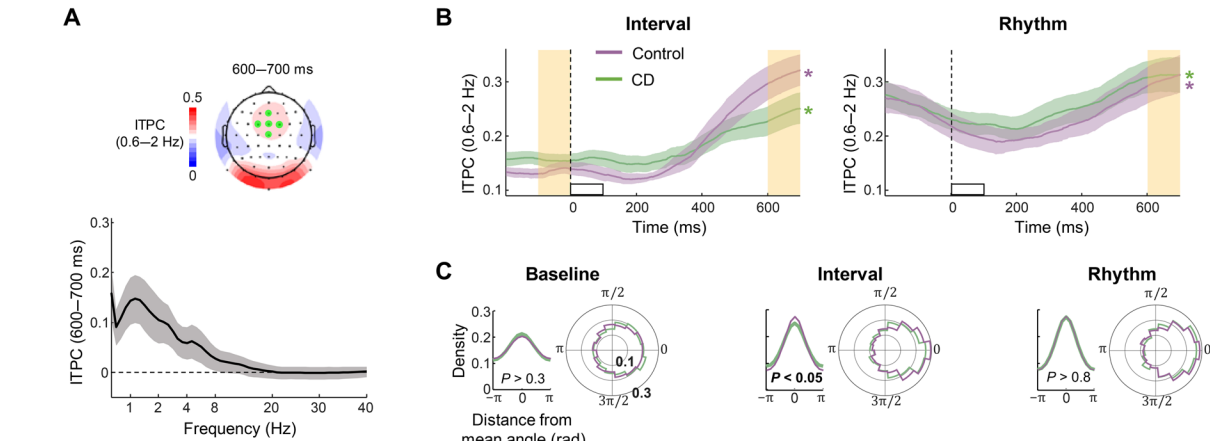


Fig. 3. Temporal alignment of neural activity depends on the cerebellum in interval-based, but not rhythm-based prediction. (A) Top: Scalp topography of delta-band (0.6 to 2 Hz) ITPC in a time window just preceding the short interval target (predefined, 600 to 700 ms after the warning signal). Green dots mark the predefined fronto-central electrode cluster used for the ITPC analysis. Bottom: Frequency distribution of ITPC across groups and tasks. Error margins indicate 95% confidence interval (uncorrected). ITPC peak is centered on the delta band. (B) Delta ITPC time-series, locked to the warning signal onset (white square) for the two tasks and groups. Target anticipation is associated with ITPC increase from baseline in both tasks and groups. Error margins indicate 1 SEM of the difference from baseline. Yellow bars mark the baseline period (left in the left panel) and pretarget window for analysis (right in both panels). * $P < 0.05$ for difference against baseline. (C) Phase distributions of delta-filtered neural activity in the baseline phase (left), and pretarget window for the Interval (middle) and Rhythm (right) tasks. The control group exhibits stronger ITPC than the CD group in the Interval task only.

interval-based mechanism. We next used a modeling approach to ask how an increase in ITPC might arise from a non-oscillatory, ramping mechanism. We simulated a set of trials using the two-parameter ramping model described above and conducted an ITPC analysis, similar to how we treated the EEG data (Fig. 4A). We first examined the spectral specificity of ITPC from the ramping model, filtering the data into a broad frequency range (0.5 to 40 Hz). ITPC from the simulated data had a frequency distribution that was centered on the delta range (Fig. 4B), matching that observed in the EEG data (compare with Fig. 3A).

As ITPC is essentially a measure of variability, we examined the impact of variability in ramping activity on delta-band ITPC (see fig. S2). For this purpose, we filtered the simulated trials (0.6 to 2 Hz) and compared simulations in which we manipulated the inter-trial variability of ramping onset latency for different levels of variability in ramping slope (Fig. 4C). As expected, ITPC decreased with larger inter-trial variability in ramping onset latency [$t(74) = -6.2, P = 0.008$]. ITPC was not affected by variation in the variability in ramping slope [$t(74) = -1.04, P = 0.3$].

Given the selective effect of onset latency on ITPC, we conducted an unrestricted spectral analysis of this variable, to examine whether the frequency distribution of ITPC effects predicted by the model matches the one in the EEG data. Simulations revealed that ITPC decrease due to increased variability in onset latency was restricted to delta frequencies (Fig. 4D, left). We then turned back to the EEG data, applying the same unrestricted spectral analysis. We focused on the Interval task given that the ITPC attenuation was observed in the CD group on this task. In line with the prediction of the model, ITPC decrease in patients with CD was limited to delta frequencies (Fig. 4D, right). Thus, countering the idea that ITPC modulations selectively reflect oscillatory alignment, a reduction in ITPC can also reflect reduced temporal consistency of the latency of ramping activity. We conjecture that this might underlie the pattern observed in the CD group.

This conjecture raises the hypothesis that individual differences in ITPC would be correlated with the cue effect on CNV latency: Higher ITPC should occur for participants who are better in adjusting the timing of the CNV. To test this, we used the model fits of the neural data to extract estimates of the cue effect on CNV latency for each participant. We found that, when controlling for group and task differences, individual differences in this metric predicted the magnitude of ITPC [linear mixed-effects (LME) regression, $\chi^2(1) = 5.34, P = 0.021$; Fig. 4E].

Timed suppression of beta activity is impaired in CD in interval-based but not rhythm-based prediction

Beta-band activity is associated with the transition from motor preparation to movement initiation, and its amplitude decreases before a temporally predictable imperative stimulus (7, 15–17). We tested the dependence of this on the cerebellum by conducting a time-frequency analysis, asking whether beta-band amplitude would be reduced before the early target time following the short SOA cue compared to the long SOA cue. Beta-band activity was analyzed in a predefined time-frequency window (see fig. S4 for frequency range identification), as well as with a two-dimensional cluster-based permutation test.

Across groups and tasks, beta amplitude was lower following the short SOA cue [cue effect, omnibus mixed ANOVA: $F(1,28) = 16.6, P = 3 \times 10^{-4}, \eta_p^2 = 0.37$], with a typical central-parietal distribution (Fig. 5A). The cue effect was different between the two groups [Cue SOA \times Group interaction: $F(1,28) = 4.56, P = 0.042, \eta_p^2 = 0.14$], although the three-way interaction of Group \times Task \times Cue SOA did not reach significance [$F(1,28) = 1.14, P = 0.15, \eta_p^2 = 0.04$]. Despite the absence of a three-way interaction in the omnibus test, we performed planned contrasts within each task to test the a priori hypothesis that the CD group would show abnormality in the Interval task but some degree of modulation in the Rhythm task. As predicted, the cue effect was smaller in the CD group on the Interval task

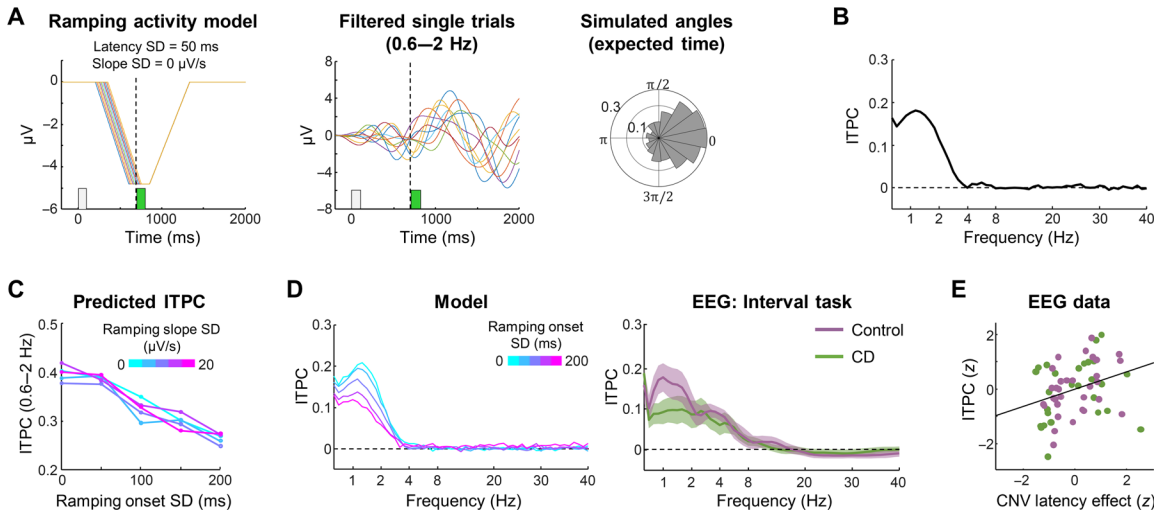


Fig. 4. Consistency of ramping activity can yield low-frequency ITPC in response to aperiodic events. (A) Modeling ITPC dependence on temporal variability of ramping activity. Left: Simulated ramping activity elicited following the warning signal (white square), with return to baseline after target onset (green square), for a set of trials with no variability in slope and low variability in onset latency. Middle: Same simulated trials, band-pass-filtered to the delta range (0.6 to 2 Hz). Right: Circular distribution of phase angles just before target time in the simulated trial set. (B) Frequency distribution of ITPC increase relative to baseline (horizontal dashed line) predicted by the ramping model. The model replicates the frequency distribution in the data (compare with Fig. 3A). (C) Predicted ITPC levels in simulated trial sets as a function of the inter-trial variability in ramping onset latency and in ramping slope. ITPC depends on the magnitude of variability in ramping onset latency. (D) Frequency distribution of ITPC increase from baseline. Left: Predictions of ramping model, as a function of the inter-trial variability in ramping onset latency. Right: EEG data from the Interval task, using the same time window as in (A). ITPC reduction is observed in the delta range, in line with the model prediction. Error margins indicate 95% confidence interval (uncorrected). (E) Between-participant correlation between ITPC and the difference of the CNV latency between the short and long cue SOAs. Purple, controls; green, patients with CD.

[Group × Cue SOA interaction, predefined window: $F(1,28) = 4.41$, $P = 0.04$, $\eta_p^2 = 0.14$, cluster-based permutation $P < 0.05$; Fig. 5B]. Analyses within each group (Fig. 5, C and D) revealed that the cue effect was significant in controls [$t(13) = -2.59$, $P = 0.022$, $d = 0.69$, cluster $P < 0.05$], but not in the CD group [$t(15) = -0.08$, $P = 0.94$, $d = 0.02$, $BF_{10} = 0.26$, moderate evidence for the null hypothesis, strongest cluster $P > 0.5$].

In contrast, in the Rhythm task, the magnitude of the cue effect did not differ between the two groups [$F(1,28) = 0.98$, $P = 0.33$, $\eta_p^2 = 0.03$; strongest cluster $P > 0.5$; Fig. 5E]. Analyses within each group (Fig. 5, F and G) revealed a cue effect in controls [$t(13) = -3.35$, $P = 0.01$, $d = 0.89$; cluster $P < 0.05$; Task × Cue SOA interaction: $F(1,13) = 0.01$, $P = 0.93$, $\eta_p^2 < 0.01$, strongest cluster $P > 0.5$]. This was also observed in the CD group [$t(15) = -2.39$, $P = 0.03$, $d = 0.6$; cluster $P < 0.05$], and the effect was stronger in the Rhythm task compared to the Interval task in the cluster-based analysis ($P < 0.05$), but not the predefined window [$F(1,15) = 1.88$, $P = 0.19$, $\eta_p^2 = 0.11$]. Thus, the CD group was impaired in timed suppression of beta-band activity in interval-based predictions, but no such impairment was observed for rhythm-based predictions.

CD results in reduced target-evoked P3 response in interval-based but not rhythm-based prediction

We next turned to a neural signature of target processing, focusing on the P3, a parietal-maximum positive polarity event-related potential (ERP) associated with stimulus evaluation and response selection (52, 53). The P3 is typically enhanced when a temporal prediction is confirmed relative to when a stimulus occurs at an unexpected time (8, 54). For this measure, we analyzed activity in a parietal electrode cluster, in a predefined time window (Fig. 6A), as well as with a cluster-based permutation test.

Across groups and tasks, the P3 response was enhanced on valid, relative to invalid trials [mixed ANOVA: $F(1,28) = 35.9$, $P = 2 \times 10^{-6}$, $\eta_p^2 = 0.56$; Fig. 6A], and the magnitude of this effect differed for the two tasks [Cue Validity × Task interaction: $F(1,28) = 8.38$, $P = 0.007$, $\eta_p^2 = 0.23$]. The Group × Task × Cue Validity three-way interaction was not significant [$F(1,28) = 0.97$, $P = 0.17$, $\eta_p^2 = 0.04$]. We used our planned contrasts to test, within each task, our a priori hypothesis regarding abnormality in the CD group. In the Interval task, the P3 enhancement was smaller in the CD group in the Interval task [Group × Validity interaction: $F(1,28) = 5.66$, $P = 0.024$, $\eta_p^2 = 0.17$; Fig. 6B]. Analyses within each group revealed that the control group displayed a significant P3 enhancement [predefined window: $t(13) = 3.43$, $P = 0.005$, $d = 0.92$; cluster $P < 0.05$], but the CD group did not [$t(15) = 1.88$, $P = 0.08$, $d = 0.47$; cluster $P > 0.05$].

In contrast, in the Rhythm task, there was no significant difference in the magnitude of P3 enhancement between groups [$F(1,28) = 0.41$, $P = 0.53$, $\eta_p^2 = 0.01$; Fig. 6C]. Analyses within group revealed P3 enhancement in controls [$t(13) = 4.2$, $P = 0.001$, $d = 1.12$; cluster $P < 0.05$] and no difference in the size of this effect between tasks [Task × Cue Validity interaction: $F(1,13) = 1.36$, $P = 0.26$, $\eta_p^2 = 0.09$]. The CD group also showed P3 enhancement [$t(15) = 3.68$, $P = 0.002$, $d = 0.92$, cluster $P < 0.05$], with the effect larger in the Rhythm task [$F(1,15) = 10.41$, $P = 0.006$, $\eta_p^2 = 0.41$].

Relating anticipatory neural dynamics to behavior

We took a two-stage approach to look at the relationship between the anticipatory neural dynamics and behavioral performance. As an initial stage, we asked whether trial-to-trial variability in CNV and beta-band predicts RT, regardless of the temporal cue. To analyze this question, we extracted single-trial CNV amplitude and beta-band amplitude (the other measures cannot be obtained from single-trial

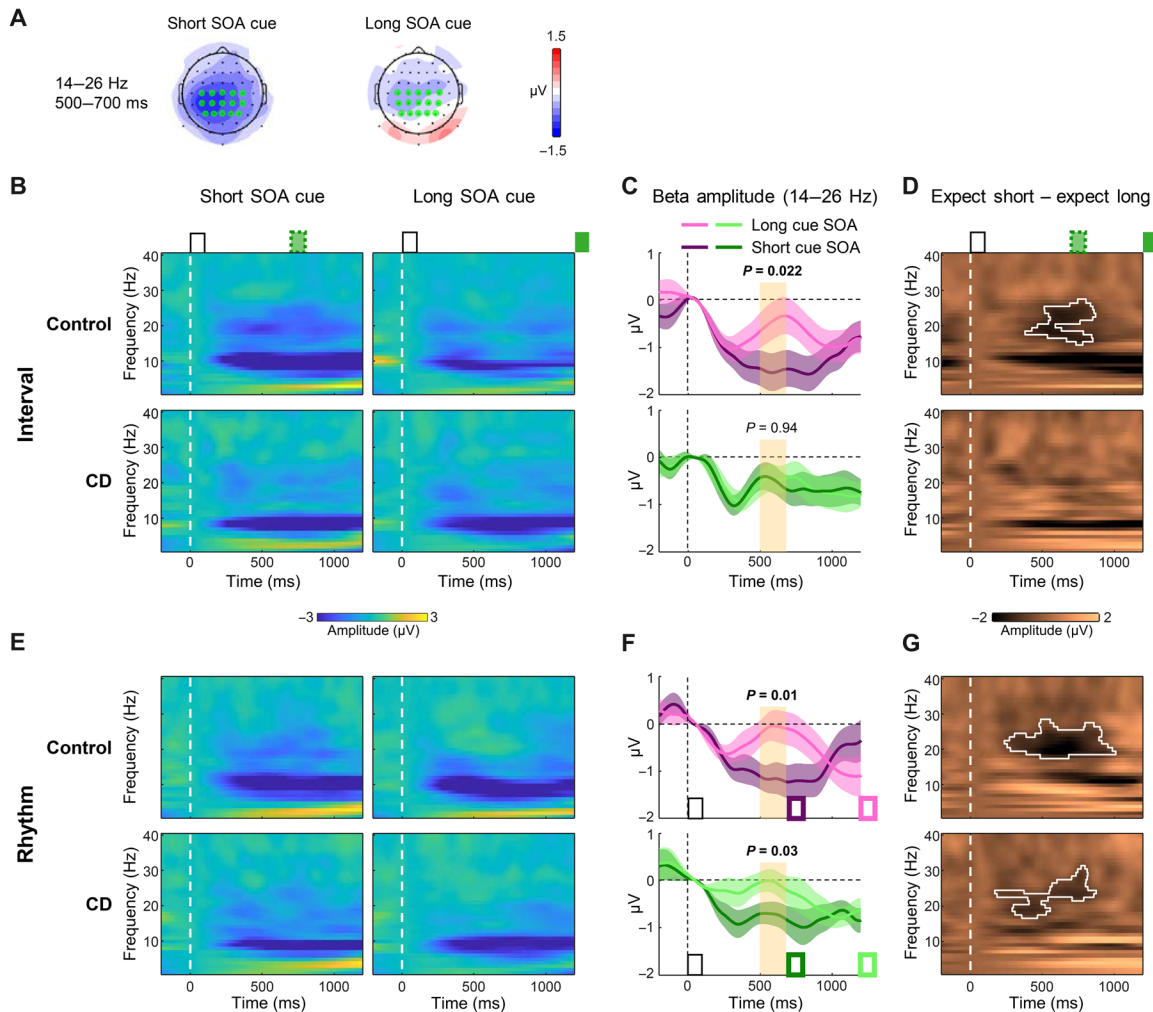


Fig. 5. Timed suppression of beta-band activity depends on the cerebellum in interval-based but not rhythm-based prediction. (A) Scalp topography of beta-band (14 to 26 Hz) amplitude in a time window just preceding the short interval target (500 to 700 ms after the warning signal). Green dots mark the predefined central-parietal electrode cluster used for the beta-band analyses. (B) Time-frequency amplitude representations in the Interval task for the control (top) and CD groups (bottom), referenced to a prewarning signal baseline period. Left: short cue SOA, target omitted. Right: long cue SOA. Vertical dashed line indicates warning signal onset. Both groups show amplitude decrease in a broad frequency range. (C) Beta amplitude (14 to 26 Hz) dynamics in the Interval task for the control (top) and CD groups (bottom). Around the short SOA target time, beta amplitude is decreased following short cue SOA in the control group, but not in the CD group. Error margins indicate 1 SEM of the difference between cue SOAs. Yellow bars mark the time window for analysis. (D) Time-frequency representations of the amplitude difference between expecting the target at short and long SOAs. A significant cluster in the beta range is only found for the controls (outlined in white, $P < 0.05$). The vertical dashed line indicates warning signal onset. (E to G) Same as (B) to (D) for the Rhythm task. Both groups show amplitude decrease in the beta range following short relative to long SOA cues.

data). Both neural signatures predicted single-trial RT (LME regression controlling for group, task, and cue SOA variability): Faster RTs were associated with larger CNV amplitude [i.e., more negative relative to baseline, $\chi^2(1) = 10.83, P = 0.001$], as well as with stronger beta-band suppression [i.e., lower amplitude relative to baseline, $\chi^2(1) = 5.49, P = 0.019$] (55–57). However, no significant correlation was found between single-trial variability in these two neural measures [$\chi^2(1) = 0.03, P = 0.86, \text{BF}_{10} = 0.024$, strong evidence in favor of the null hypothesis].

Having confirmed that these measures are predictive of behavior, we next turned to a between-subject analysis, looking at the relationship between the impact of temporal anticipation on behavioral performance and anticipatory neural dynamics. To quantify the for-

mer, we used the RT validity effect. To quantify the latter, we used the cue effect, the difference between the short and long cue SOA conditions for the CNV amplitude, CNV latency, CNV slope, and beta-band amplitude. For ITPC, we took the magnitude of increase from baseline, collapsing across the cue SOA conditions. An LME regression model was used to control for group and task differences (fig. S5).

For the CNV amplitude, the size of the cue effect was not significantly correlated with the validity effect [$\chi^2(1) = 1.84, P = 0.17$]. However, when we used the parameters from the CNV model, the cue effect on both CNV latency and slope was positively correlated with the validity effect [latency: $\chi^2(1) = 6.59, P = 0.01$; slope: $\chi^2(1) = 3.96, P = 0.046$]. The size of the cue effect was also correlated

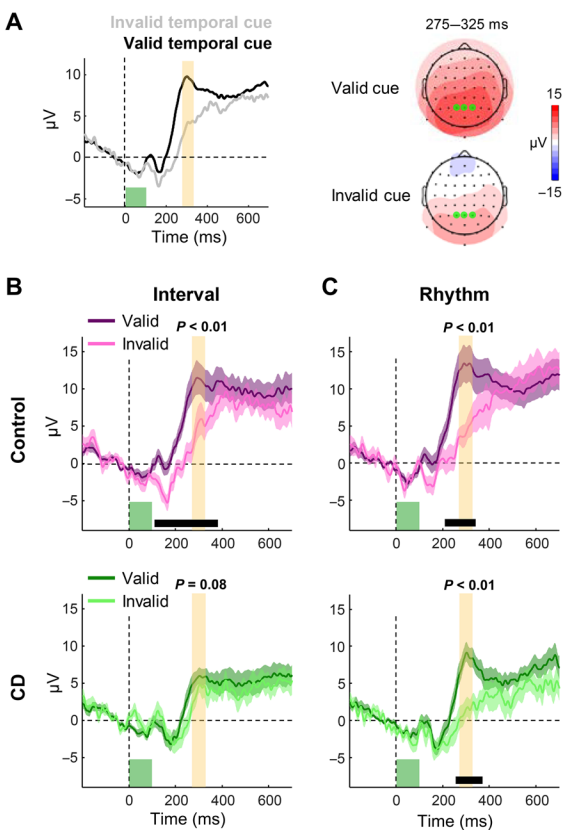


Fig. 6. P3 enhancement depends on the cerebellum in interval-based but not rhythm-based prediction. (A) ERPs time-locked to target onset (green square) on valid (dark) and invalid (light) trials, averaged across groups and tasks. The P3 response is enhanced on valid trials. Scalp distribution depicted for a time window surrounding the P3 peak. Yellow bars on the waveform plots mark the time window used to plot the scalp distributions and for subsequent analyses (275 to 325 ms after the target). Green dots mark the predefined parietal electrode cluster used for the P3 analysis. (B) P3 in the Interval task for the two groups in valid trials (dark color) or invalid trials (light color). P3 enhancement on valid trials is only observed in the control group (top) but not in the CD group (bottom). Error margins indicate 1 SEM of the difference between expected SOAs. Yellow background indicates the predefined window for analysis following target onset. Horizontal bars indicate clusters of consecutive time points with significant difference between conditions. (C) Same as (B) for the Rhythm task. P3 enhancement on valid trials is observed in both groups.

with the validity effect for beta-band activity [$\chi^2(1) = 5, P = 0.025$], such that a larger cue effect was associated with a larger validity effect, but not with the magnitude of ITPC increase [$\chi^2(1) = 0.17, P = 0.68$].

When looking at the correlation between the physiological signatures, the cue effects for the slope and latency parameters were correlated, with smaller latency difference associated with steeper slopes after short cues [$\chi^2(1) = 116.83, P = 3 \times 10^{-16}$]. The cue effect on beta-band amplitude was not correlated with the adjustments of CNV latency, CNV slope, or raw CNV amplitude (all P 's > 0.05). ITPC was correlated with the CNV latency (see above), but not with the other EEG measures (P 's > 0.05).

Overall, several signatures of anticipatory neural dynamics were correlated with behavior, manifest in both single-trial and individual difference analyses. Other than the correlation between ITPC and CNV latency, we did not observe correlations between the physiological signatures.

DISCUSSION

Our results reveal a critical role for the cerebellum in the control of the neural dynamics associated with temporal prediction in an attentional orienting task (1, 2). When temporal predictions were based on an interval-based representation, CD impaired several EEG signatures of temporal anticipation, including the CNV, beta-band activity, and phase locking of low-frequency activity. When the expected interval was cued using a periodic stream of stimuli, these same neural signatures were preserved. Echoing this dissociation, the CD group also showed diminished behavioral facilitation as well as an attenuation of the target-evoked P3 response to valid targets in interval-based prediction, but a normal response in rhythm-based prediction. Going beyond the group differences, we also found that the modulation of the physiological measures predicted the behavioral benefit from temporal cues, corroborating the involvement of these neural patterns in temporal attention. Together, these results presented here establish a causal role of the cerebellum in the adjustment of anticipatory neural dynamics associated with interval-based temporal prediction. Moreover, the dissociations between interval- and rhythm-based predictions indicate that these neural adjustments are not unique to periodic or aperiodic contexts, but can be driven by distinct mechanisms in different contexts.

The starting premise for this study is that temporal anticipation entails adjustment of dynamic activity across a cortico-striatal network (3, 7, 9, 11, 19, 20, 58). Our primary goal was to identify how the cerebellum influences cortico-striatal dynamics by observing how CD affects EEG-based signatures of temporal anticipation (see Fig. 1A). We observed CNV buildup, beta suppression, and delta ITPC increase in the CD group in response to both types of cues, evidence at odds with the hypothesis that the cerebellum is essential in the generation of these anticipatory signals. However, in the Interval task, the CD group showed no effect of cue SOA on the CNV or beta-band activity and reduced delta ITPC. Thus, the results are consistent with the cerebellar-dependent adjustment model: Integrity of this subcortical structure is required to modulate anticipatory neural dynamics as a function of the expected interval when the prediction relies on an interval representation.

It is important to emphasize that we do not claim that the EEG signals described here directly reflect cerebellar activity. As noted above, evidence from multiple methodologies indicates that these signals reflect activity in cortico-striatal networks. Furthermore, recent work suggests that EEG recordings only capture high-frequency cerebellar activity (>75 Hz) (59). Thus, EEG abnormalities in the CD group presumably reflect the downstream consequences of altered or absent cerebellar input.

In terms of functional interpretation, the CNV and beta activity have been associated with different processing stages. The CNV is observed on both motor and nonmotor tasks (60–62). Consequently, it has been interpreted as reflecting an increase in excitability in preparation for an upcoming event, independent of the response to that event (62, 63). In contrast, suppression of beta-band activity over sensorimotor regions is observed during motor execution and anticipation of movement cues (64, 65), suggesting that it reflects increased motor readiness (66, 67). Consistent with the assumption that the CNV and beta-band activity reflect nonoverlapping functional stages, we did not observe a correlation between the two physiological measures, in both the single-trial and individual differences analyses. Our results underscore that when temporal predictions rely on interval representation, the cerebellum is critical for multiple functional components of temporal anticipation.

The notable dissociation between the Interval and Rhythm tasks has several important implications. Methodologically, it suggests that the CD group's EEG abnormalities in the Interval task are unlikely to reflect inferior data quality that might be related to degenerative processes. Theoretically, the dissociation further corroborates the functional separation between interval-based and rhythm-based prediction (28) and specifies an important boundary constraint on cerebellar contributions to prediction and timing [but see (68, 69)]. Moreover, it indicates a separation between processes that are involved in the generation of anticipatory neural patterns and processes that modulate these signals in a context-specific manner. Specifically, the present results provide evidence that modulation of the CNV, beta-band activity, ITPC, and P3 in periodic streams does not reflect a single mechanism operating in both contexts. Rather, these physiological signatures reflect shared downstream processes that are temporally adjusted based on context-specific input such as cerebellar-dependent interval representations. We note that the three-way interactions were not significant for beta and the P3; however, in both cases, the CD group remained insensitive to the duration of the cue in the Interval task.

The one exception for this context specificity was that the CD group failed to show an SOA-dependent adjustment in the latency of ramping activity in both the Interval and Rhythm tasks. These results imply that the cerebellum is critical for modulating the onset timing of neural preparation independent of context. Consistent with this idea, neural recordings in NHPs reveal that, when the delay before a cued movement is varied, ramping activity in the cerebellum changes in onset latency but not slope. The reverse is observed in the striatum where the slope varies, but not the latency (37, 38). It may be that when the ability to control latency is compromised as in the CD group, some degree of compensation is possible by adjusting the slope of the ramping activity if the input engages striatal computations associated with rhythmic prediction (28).

Unlike the correlational nature of most neuroimaging work, neuropsychological studies can provide an opportunity to make causal inferences, asking how damage to a particular structure affects behavior, and in the current study, electrophysiological correlates of that behavior. We recognize that there are limitations in making claims about causality, especially when the evidence is based on a single dissociation. For example, it is possible that the Rhythm task is less demanding than the Interval task. However, our control group, and two previous studies (6, 28), showed similar behavioral and neural adjustments for interval- and rhythm-based prediction. Moreover, we had, *a priori*, anticipated the observed dissociation: The interval-specific hypothesis arose from our previous behavioral work in which we observed a double dissociation, such that individuals with Parkinson's disease were selectively impaired in exploiting rhythmic temporal cues (28). Although we have chosen to focus on the cerebellum in this study, previous work from other laboratories has shown that PD is associated with impairments in CNV modulation and beta-band attenuation based on rhythm-based predictions (70–72); future work should examine these measures in response to interval cues. At present, the dissociation within the CD group points to an asymmetric role of the cerebellum in these two modes of prediction and implies that the neural signatures of predictions do not rely on the cerebellum across contexts.

Whether temporal prediction relies on oscillatory entrainment is controversial, as is the interpretation of ITPC as a measure of rhythm-specific mechanisms such as entrainment (42–46). Two

results in the current study are relevant to this debate. First, the finding that the CD and control groups showed a similar change in ITPC in the Rhythm task argues against the idea that ITPC in rhythmic streams arises from an interval-based mechanism; indeed, ruling out this explanation of ITPC provides indirect support for an entrainment account of rhythm-based prediction. Second, the attenuation of ITPC in the CD group in the Interval task indicates that an increase in ITPC need not require a rhythm-based mechanism but, rather, can result from an interval-based prediction. Thus, we propose that an increase in ITPC reflects the operation of different mechanisms when predictions are based on rhythmic streams or an interval-based representation, with the latter depending on the cerebellum. As shown by the modeling work, the decrease in ITPC in the Interval task for the CD group can be accounted for by assuming an increase in variability of the onset latencies of nonoscillatory ramping activity. Moreover, across participants, the magnitude of ITPC correlated with the cue effect in latency adjustment of the CNV, pointing to a possible shared computation related to latency control. We note that the fact that ITPC can reflect ramping activity in isolated interval contexts does not reject the possibility that it reflects oscillatory entrainment in rhythmic streams. Strong evidence for involvement of oscillatory mechanisms would require observing oscillatory patterns that cannot be explained by interval-based prediction, such as reverberation after stream termination (6, 73, 74).

Our results speak against a generalized cerebellar role in attentional anticipation, motor preparation, prediction, or rapid neural coordination (38, 75, 76). Instead, cerebellar computation appears to be specific to prediction in an interval-based context. Similar cerebellar selectivity to interval-based timing is also observed in other timing domains. In timed movement, CD impairs discrete tapping but not circle drawing, where the latter might be achieved by transforming the temporal goal into a velocity-based signal (33). In explicit timing judgments, CD impairs interval discrimination but not beat identification (29, 31). Similar dissociations between isolated interval timing and more continuous forms of timing have been reported in neuroimaging studies (30, 34).

Computationally, it has been proposed that the cerebellum is critical for timing isolated intervals that are defined by salient events ("event timing"), but not when temporal representation is inherent to the ongoing dynamic context ("emergent timing") (77). Our results underscore that this constraint is not limited to tasks involving explicit temporal representation but also applies to temporal anticipation tasks in which timing is implicit. The current results indicate that the cerebellum controls interval-based temporal predictions by adjusting the latency of anticipatory processes. When intact, this cerebellar-dependent adjustment process would support more cost-effective resource allocation, allowing an appropriately tuned neural state at the expected time.

This hypothesis makes explicit that the neural circuitry underlying temporal prediction entails multiple levels of information processing. Adjustments of the CNV, beta activity, and delta ITPC reflect processes related to the control and implementation of attentional and motor preparation (1), independent of context. However, to be optimized, these signals require modulatory inputs; in an interval context, the cerebellum provides the context-specific representations of time (32). In other contexts, such as rhythmic streams, the representation of time, as well as manner in which neural dynamics for temporal anticipation are modulated, might rely on other structures such as the striatum (28, 78). Consistent with this hypothesis,

temporal adjustment of the CNV and beta activity in these contexts is not impaired by cerebellar dysfunction, but by striatal dysfunction (71, 72).

To conclude, our results indicate that the neural dynamics of attentional anticipation in the time domain critically relies on the cerebellum in a context-specific manner, one in which prediction arises from an interval-based representation. The findings not only advance our understanding of the functional domain of the cerebellum in timing but also necessitate updating our understanding of neural signatures of temporal prediction. While these signals may originate in extracerebellar circuits, the ability to fine-tune the timing of these neural dynamics is dependent on cerebellar representations in the absence of a periodic context. When coupled with previous work on temporal judgment, reproduction, and sensorimotor learning (79–81), we begin to have a coherent picture of the unique role of the cerebellum in temporal attention.

MATERIALS AND METHODS

Participants

Eighteen patients with CD and 16 neurotypical control individuals were recruited for the study. The data from two individuals from each group were discarded because of excessive noise in the EEG recordings or an inability to perform the task, leading to a final sample size of 16 individuals with CD and 14 controls. The study was approved by the Institutional Review Board at the University of California, Berkeley, and all of the participants provided informed consent. They were financially compensated for their participation.

Participants in the CD group (10 females, 15 right-handed, mean age = 56.7 years, SD = 11.4) had been diagnosed with spinocerebellar ataxia, a slowly progressive adult-onset degenerative disorder in which the primary pathology involves atrophy of cells within the cerebellum. We did not test patients who presented symptoms of multisystem atrophy. Eleven individuals in the CD group had a specific genetic subtype (SCA1 = 1, SCA3 = 5, SCA5 = 1, SCA6 = 2, SCA8 = 1, and SCA10 = 1), and the other five individuals had CD of unknown/idiopathic etiology. All of the participants with CD completed a medical history interview to verify the absence of other neurological conditions and were evaluated at the time of testing with the Scale for the Assessment and Rating of Ataxia (SARA) (82). The mean SARA score was 11.8 (range, 3.5 to 25.5; SD = 6.6). Control participants (8 females, 13 right-handed, mean age = 60.4, SD = 9.2) were recruited from the same age range as the CD group and, based on self-reports, did not have a history of neurological or psychiatric disorders. The CD and control groups did not differ significantly in age ($P = 0.34$).

All participants were prescreened for normal or corrected-to-normal vision, intact color vision, and no professional musical training or recent amateur participation in musical activities (e.g., playing a musical instrument or singing in a choir). All of the participants completed the Montreal Cognitive Assessment (MoCA) as a simple assessment of overall cognitive competence. Although we did not select participants to provide a match on this measure, there was no significant group difference (CD: mean = 27.6, Control: mean = 28.3, $P = 0.18$).

Procedure

Upon arrival, all participants provided consent and demographic information and completed the MoCA. Participants in the CD group

also provided their clinical history (if not on file from a visit within the past year) and were evaluated with the SARA.

The experiment was conducted in a quiet, dimly lit room, with a laptop computer placed on a table in front of the participant. The stimuli (colored squares, 5 × 5 cm, 5.5°) were presented at the center of a 15-inch laptop monitor on gray background (viewing distance ≈ 50 cm). Stimulus presentation and response acquisition were handled using Psychophysics toolbox (83) for MATLAB (MathWorks).

Each trial began with the temporal cuing phase, consisting of the serial presentation of two or three red squares (stimulus duration = 100 ms). There were two types of cues, tested in separate blocks. In the Interval task, the cue consisted of two red squares, each presented for 100 ms, with an SOA of either 700 ms (short cue) or 1200 ms (long cue). In the Rhythm task, the cue consisted of three red squares, presented periodically with an SOA of 700 ms (short cue, equivalent to 1.43 Hz) or 1200 ms (long cue, 0.83 Hz). The last red square was followed by the presentation of a white square, the warning signal, indicating to the participant that the subsequent stimulus would be the target. For the Rhythm task, the interval between the last red square and warning signal was set to the same duration as the cue SOA for that trial. Thus, the warning signal fell on the “beat” established by the temporal cues. In contrast, for the Interval task, the interval between the last red square and warning signal was randomly set on each trial to be either 1.5 or 2.5 times the duration of the SOA on that trial (short cue SOA: 1050/1750 ms; long cue SOA: 1800/3000 ms). This strongly reduced any periodicity in the stimulus train and thus eliminated the use of a rhythmic strategy since the warning signal occurred at 180° phase relative to a beat that, in theory, could have been created by the two red squares (6). We favored this type of cuing over purely symbolic cuing (8, 9) to minimize the need to learn the target intervals across trials.

Starting with the onset of the warning signal, the trial events were identical for the two tasks. After a short delay, the target, a green square, was presented, and the participant was instructed to make a speeded button press using their right index finger upon detection of the target. The interval between the warning signal and target was either the same SOA as defined by the temporal cue (valid trial) or the noncued SOA (invalid trials). The cue was valid on 56.25% of the trials and invalid on 18.75% of the trials; this 3:1 ratio was selected to incentivize the participant to attend to the temporal cues to facilitate performance. On the remaining 25% of the trials, no target was presented. These catch trials were included to discourage participants from making anticipatory responses (10). Participants received feedback (error message on the monitor) if they responded prematurely, if they responded on a catch trial, or if they did not respond within 3 s of target onset.

Participants preformed four blocks of each task, each consisting of 32 trials, in alternating order (eight blocks total, first block counterbalanced across participants). Within each block, the duration of the temporal cue was randomly determined with the constraint that each cue occurred on 50% of the trials for all conditions (valid, invalid, catch). Short breaks were provided between each block. Before the first block for each task, the experimenter demonstrated the trial sequence and then conducted short blocks of practice trials ($n = 8$ trials), repeating the practice block until the participant could describe how the cues were predictive of the onset time of the target. For subsequent blocks, the participant first completed two practice trials as a reminder of the format for the temporal cues in the forthcoming block.

EEG recording and preprocessing

EEG was recorded continuously from 64 preamplified Ag/AgCl electrodes, using an Active 2 system (BioSemi, The Netherlands). The electrodes were mounted on an elastic cap according to the extended 10-20 system. Additional electrodes were placed on the outer canthi of the right and left eyes, above and below the center of the right eye to track electro-ocular activity, and on the left and right mastoids and near the tip of the nose to be used as reference electrodes. The EEG signal was sampled at a rate of 1024 Hz (24 bits/channel), with an online anti-aliasing 204-Hz low-pass filter.

EEG preprocessing was conducted in MATLAB using the FieldTrip toolbox and custom-written scripts. We used the following analysis pipeline: (i) referencing to average of right and left mastoid electrodes; (ii) high-pass filtering using a zero-shift Butterworth filter with a cutoff of 0.1 Hz (24 dB/octave); (iii) correction of ocular artifacts using independent component analysis (84) based on typical scalp topography and time course; (iv) elimination of epochs that contained artifacts that were noncognitive in origin (defined as absolute activity larger than 100 μ V or a change of more than 100 μ V in a 200-ms interval).

Behavioral data analysis

Trials were discarded if a response was detected before target onset or if the RT was shorter than 100 ms or longer than 3000 ms (2.2% of trials, no difference between groups or tasks). From the remaining trials, we discarded those with RT of more than 3 SDs above or below the mean RT, calculated separately for each of the conditions. Only 0.7% of all trials were rejected on this criterion, with no difference between groups or tasks.

We first conducted an omnibus mixed ANOVA with factors Group (CD/Control), Task (Interval/Rhythm), Target SOA (Short/Long), and Cue Validity (Valid/Invalid) to assess the validity effect (faster responses for valid versus invalid trials) across groups and tasks. The three-way interaction in the omnibus test also sheds light on how the validity effect varies between the two groups and two tasks. We expected that the CD group would show behavioral impairments in the Interval task and, as such, designed a series of analyses based on this prediction. To compare the validity effect between groups within each task, we conducted planned contrasts using a mixed ANOVA with factors Group, Cue Validity, and Target SOA. To assess the validity effect within each task and group, we conducted planned contrasts using a repeated-measures ANOVA with factors Cue Validity and Target SOA. To assess context specificity within each group, that is, compare the validity effect between the two tasks, we used a repeated-measures ANOVA with factors Task, Target SOA, and Cue Validity. Here, and in all subsequent analyses, effect sizes were estimated using Cohen's d and partial eta-squared (η_p^2). For comparisons in which we predicted no difference between conditions, evidence in favor of this null hypothesis was tested by calculating the Bayes factor in JASP (JASP Team).

ERP analysis

All EEG analyses were conducted in MATLAB using custom-written scripts and the CircStat toolbox (85). Analysis of anticipatory ERP components focused on the CNV, a negative polarity potential arising in the interval between the warning signal and an expected target, which typically peaks just before the anticipated event (6–8). For the CNV analysis, continuous EEG data were segmented into epochs extending from 200 ms before to 700 ms after warning signal stimuli,

and these were averaged separately for each participant, task, and expected SOA. The 100-ms epoch just before the warning signal was used as the baseline. Given that the early target would occur 700 ms after the warning signal, we predicted that the CNV would have a larger amplitude (i.e., be more negative) following the short temporal cue, relative to the long temporal cue.

Analysis of a target-evoked ERP focused on the P3 response, whose amplitude is typically enhanced following valid compared to invalid temporal cues (8, 54). Note that while temporal prediction was also found to affect early sensory EEG responses, these effects are only observed in demanding perceptual tasks (61), but are typically absent in supra-threshold detection tasks such as that used here. For the P3 analysis, segments extending from 200 ms before to 700 ms after target onset were averaged separately for each participant, task, and cue validity, with a period of 100 ms before the target used as baseline. The P3 analysis was restricted to short SOA targets, because of well-documented baseline contamination in invalidly cued long SOA targets by CNV resolution following an omitted short SOA target (6, 7).

The CNV and P3 were analyzed in predefined fronto-central (Fz, FC1, FCz, FC2, Cz) and parietal (P1, Pz, P2) electrode clusters, respectively (6–8). Electrode selections were validated by inspecting the data across groups and tasks (Figs. 2A and 5A). To compare the CNV and P3 amplitude between conditions, the amplitude was averaged for each participant across a predefined time window (CNV, 600 to 700 ms after the warning signal, just before the short SOA target; P3, 275 to 325 ms after the target, around the expected peak latency based on the literature and an informal assessment of our data set across conditions).

For each of these neural measures, we first conducted an omnibus mixed ANOVA with factors Group (CD/Control), Task (Interval/Rhythm), and Cue SOA (Short/Long), with the three-way interaction shedding light on how the measures vary between the two groups and two tasks. Given the expected behavioral impairment in the CD group on the Interval task, we designed a series of analyses based on the prediction that this impairment would be associated with selective abnormalities in some or all of the neural signatures of temporal anticipation. Within each task, we conducted planned contrasts using a mixed ANOVA with factors Group and Cue SOA to compare the modulation of each ERP by the cue duration between groups. Within each task and group, we conducted planned contrasts to test the effect of cue SOA on the CNV and P3 amplitudes, using paired t tests. To assess context specificity within each group, we used a repeated-measures ANOVA with factors Task and Cue SOA.

We also used a cluster-based permutation test to evaluate the temporal extent of the difference between conditions without restriction to a predefined window (48) (10,000 iterations, shuffling conditions within participants, individual time point threshold: $P < 0.05$). Randomization test P value can vary slightly with repeated application of the analysis because of the arbitrary shuffling. As such, here and in subsequent permutation analyses, P values are reported as lower than a significance threshold.

To quantify how the CNV was affected by CD in each task, we fit the CNV waveform observed between the warning signal and the time of the short SOA target (700 ms) with a two-parameter model of ramping activity (Fig. 2D). The model approximates a climbing neuronal activity process (86, 87), assumed to have linear ramping (slope, S) with a variable onset time (T) as follows

$$Amp(t) = \begin{cases} 0 & \text{if } 0 < t \leq T \\ S * (t - T) & \text{if } T < t \leq 700 \end{cases}$$

This model was fit to the data of each group, task, and cue SOA condition using the “fminsearch” function in MATLAB (Nelder–Mead simplex optimization) with several initial values to minimize effects of local minima, covering a biologically plausible range of parameters ($T = 0$ to 700 ms, $S = 0$ to $-350 \mu\text{V/s}$). We averaged across participants in each group given that the high levels of noise in single-subject data would lead to unstable fits.

To confirm that the extracted model parameters capture variability in the measure of raw CNV amplitude, we examined whether individual differences in the cue effect on the two parameters (e.g., latency difference between short and long cue SOA conditions) predict individual differences in the cue effect on CNV amplitude. As the model was only fit to group-averaged waveforms, we used a jackknifing procedure (88) to obtain single-subject approximations of the cue effect on the latency and slope parameters. An LME regression model was then used to predict the size of the cue effect on CNV amplitude from the cue effect on the two model parameters simultaneously (because of the high correlation between them, see Results), controlling for group and task differences. This analysis revealed a joint effect of the two parameters [$\chi^2(2) = 8.07, P = 0.018$], confirming that the model provides a reasonable account of how temporal anticipation influences the CNV.

To compare the model parameters between conditions, we used a permutation-based approach for each parameter. For each effect of interest, we estimated the difference between conditions observed in the true unshuffled data. We compared this value to a null distribution, created by shuffling the appropriate condition labels, averaging according to the shuffled labels, fitting the model to group-averaged waveforms, and calculating the difference between parameters on these shuffled datasets (5000 iterations). The difference between conditions was considered significant only if it was larger than the difference obtained in 95% of the randomized datasets. To assess the effect of cue SOA across all conditions (i.e., short versus long, termed cue effect), the null distribution was created by shuffling cue SOA labels within each group and task. A similar shuffling protocol was used to test the cue effect within each group and task (equivalent to simple effect of the Cue SOA factor). To compare the cue effect between groups (equivalent to a Group \times Cue SOA interaction), the null distribution was created by shuffling group labels between participants within task. To compare the cue effect between tasks (equivalent to a Task \times Cue SOA interaction), the null distribution was created by shuffling task labels within participants. Last, to compare group difference in cue effect between tasks (equivalent to a three-way Task \times Group \times Cue SOA interaction), the null distribution was created by shuffling cue SOA and task labels within participants and group labels across participants.

Time frequency analysis

For the time frequency analysis, we focused on modulations in the delta and beta bands. In the delta band, temporal prediction is associated with increased ITPC (51) in anticipation of a target (3, 4, 6), in both periodic and aperiodic streams (6, 42, 43). For the ITPC analysis, we band-pass-filtered the data in the delta-frequency range (0.6 to 2 Hz Butterworth filter, 24 dB/octave), extracted the instantaneous phase using the Hilbert transform, and calculated the ITPC (fig. S2). The 0.6- to 2-Hz frequency range was chosen as it is roughly

symmetric (logarithmically) around the frequencies that correspond to the short and long target intervals (700 ms = 1.43 Hz and 1200 = 0.83 Hz; ~0.5 octave margins from each side). We used a causal filter (instead of a noncausal zero-lag filter) to avoid contamination of the anticipatory period by target-evoked activity.

To examine the effect of CD on ITPC modulation by temporal prediction, we applied this analysis pipeline to the EEG data from the same fronto-central region of interest as used in the CNV analysis (Fz, FC1, FCz, FC2, Cz). By using the same electrodes, we were in a position to examine whether temporal variability across trials is related to systematic adjustments observed in the CNV analysis. The data were segmented within an epoch extending from 200 ms before the warning signal until 700 ms after the warning signal, with ITPC calculated at each time point, separately for each group, task, and cue duration. Given that we did not expect to observe a difference in this measure between the two temporal cue conditions, we averaged the results across this factor. We focused on ITPC levels just before the early target by averaging across a predefined window of 600 to 700 ms after the warning signal. These values were baseline-corrected and then compared between groups. For the baseline, ITPC values were averaged across the 100-ms epoch just before the onset of the warning signal. The prewarning signal period from the Interval task was used as baseline for both tasks, given that, in the Rhythm task, the warning signal is also temporally predictable. Since ITPC values are not normally distributed, we used nonparametric permutation tests, comparing observed ITPC differences to a null distribution of randomized ITPC differences (5000 iterations). We used a permutation-based *t* test comparing all participants against baseline to test for an ITPC increase. A similar approach was used to test for an ITPC increase within each group. To compare ITPC between groups within each task, we used a between-subject permutation test in which we shuffled group labels. To assess context specificity in each group, we used a within-subject nonparametric permutation test in which we shuffled task labels. To compare the group difference in ITPC between the two tasks, we used a nonparametric permutation-based mixed ANOVA (50), with the factors Group and Task.

To examine whether ITPC can reflect temporal consistency of nonoscillatory ramping activity, we used a modeling approach, applying our pipeline to simulated data. We simulated a set of 60 trials (matching the approximate number of trials per condition in the actual data) using the two-parameter ramping model described above. To avoid edge artifacts, we added a stage in which the activity gradually returns to baseline after target onset (6, 7). For each set of simulated trials, ramping onset latency and slope for each trial were chosen randomly from a Gaussian distribution with a specific SD (onset latency: mean = 300 ms, SD = 0, 50, 100, 150, or 200 ms; slope: mean = $-12 \mu\text{V/s}$, SD = 0, 5, 10, 15, 20 $\mu\text{V/s}$). The range of SDs for each parameter were chosen to cover a physiologically relevant scale. The lower bounds were set to 0 (no variation) and the higher bounds were constrained to minimize the number of simulated trials exceeding the task constraints (latency values up to 700 ms, which is the target time in which the CNV ramping is terminated, and slope values that would lead to an amplitude of $\sim 5 \mu\text{V}$, the observed peak amplitude in the EEG data, after 700 ms). 1/f random noise was added to the simulated time series given its presence in EEG recordings. We then applied the ITPC pipeline used for the EEG data and extracted the ITPC just before target time. To ensure stability, the results for each of the 25 combinations of distribution SDs were averaged across 100 iterations and three amplitude levels of the 1/f noise. To examine

whether ITPC depended on the magnitude of inter-trial variability in ramping onset latency or slope, we conducted a multiple regression analysis to predict the resulting ITPC values from these two predictors (see also fig. S2).

We also evaluated the model by performing a spectral analysis in which the EEG and simulated data were filtered to encompass a wider range of frequencies (seed frequency: 0.4 to 8 Hz, 1/6 octave steps, 9 to 40 Hz, 1-Hz steps, symmetric 0.5 octave filter width around seed frequency, Butterworth filter, 24 dB/octave). For the model, we repeated this analysis while varying the SD of the latency parameter, which was found in the regression analysis to affect ITPC. For the EEG data, this analysis was conducted separately for each group in the Interval task, where ITPC reduction was observed in the CD group. To test the association between ITPC and cue effects on CNV latency, an LME regression model was used to predict individual differences in ITPC from the magnitude in latency adjustment by the expected interval (using jackknifing, see above).

The amplitude of activity in the beta band decreases before the time of an expected event that requires a motor response (7, 15–17). Thus, we expected lower beta amplitude just before the time of the early target following a short cue compared to following a long cue. To test this prediction, segments extending from 1200 ms before to 2200 ms after the warning signal were subjected to a time-frequency decomposition using a complex Morlet wavelet transform (1 to 40 Hz, 1-Hz steps, ratio between the central frequency and the SD of the Gaussian-shaped wavelet in the frequency domain = 8). We discarded the first and last 1000 ms from the analyses to exclude edge artifacts. Instantaneous amplitudes were averaged separately across trials for each participant, task, and temporal cue for each electrode. For the baseline measure of spectral amplitude, we used the 100-ms window after the warning signal (6).

Beta-band suppression is observed in central-parietal sites (7, 15, 16, 18), but there is no consensus on the appropriate frequency range for beta. To select the range for our analyses in an unbiased manner, we inspected the time-frequency representations, averaged across groups, tasks, and electrodes (fig. S4). From this grand average waveform, we identified suppression in the frequency range of 14 to 26 Hz. Examining the scalp distribution of activity in these frequencies confirmed a central-parietal focus. Therefore, we analyzed beta activity in a central-parietal electrode cluster (C3, C1, Cz, C2, C4, CP3, CP1, CPz, CP2, CP4, P3, P1, Pz, P2, P4).

To compare the beta amplitude between conditions, the amplitude was averaged for each participant across a predefined time window (500 to 700 ms after the warning signal, just before the early target time). To avoid contamination from target-evoked activity, we only included trials in which target did not appear at the early interval (invalid and catch for short cue, valid and catch for long cue). We first conducted an omnibus mixed ANOVA with factors Group (CD/Control), Task (Interval/Rhythm), and Cue SOA (Short/Long) to assess the cue effect across groups and tasks, as well as how it differs between them (focusing on the three-way interaction). To compare the impact of cue SOA on beta amplitude between groups, we conducted planned contrasts using a mixed ANOVA with factors Group and Cue SOA. Within each task and group, we conducted planned contrasts to compare the beta amplitude between short and long cue conditions, using paired *t* tests. For context specificity, we compared the cue effect between tasks within each group using a repeated-measures ANOVA with factors Task and Cue SOA. We also evaluated the spectro-temporal extent of the difference between

conditions without commitment to a predefined time or frequency window using a two-dimensional cluster-based permutation test (48) (10,000 iterations, shuffling conditions within participants, individual time threshold: *P* < 0.05).

Correlational analyses between EEG and behavioral measures

We used a two-stage approach to examine the relationship between neural signatures of temporal anticipation and behavioral performance. First, we asked whether trial-to-trial variability in the neural measures predicted behavior. Here, we examined single-trial CNV and beta amplitudes, the two measures that can be obtained for single trials, as predictors of RT, and also whether they were correlated, using LME regression. To avoid effects from prediction violations or foreperiod-related expectations, the single-trial amplitudes and RTs were only extracted from trials in which a short target interval was validly cued. CNV and beta-band amplitudes were extracted using the same time-frequency windows and electrode clusters as in the group analyses (just before the short interval target, see above) and referenced to the same baseline windows.

Second, in a between-subject analysis, we examined whether the magnitude of the cue effect (difference between short and long cue SOA conditions) for each neural marker predicted individual differences in behavior and whether the different neural markers were correlated. Predictors here included raw CNV amplitude, CNV onset latency, CNV slope, and beta amplitude. Since ITPC is a measure of variability, it should not vary with SOA; thus, we used the mean value across the two cue SOAs (as was done for the group analysis). We tested the association between each measure and the behavioral validity effect, as well as between measures, using LME regressions. The use of LME models allowed us to simultaneously use the entire dataset while controlling for group and task effects (an analysis within each group and task would have considerably less power). In both analyses, the final models included fixed effects for group and task, as well as random intercepts for participant.

SUPPLEMENTARY MATERIALS

Supplementary material for this article is available at <http://advances.sciencemag.org/cgi/content/full/6/49/eabb1141/DC1>

[View/request a protocol for this paper from Bio-protocol.](#)

REFERENCES AND NOTES

1. A. C. Nobre, F. van Ede, Anticipated moments: Temporal structure in attention. *Nat. Rev. Neurosci.* **19**, 34–48 (2018).
2. C. E. Schroeder, P. Lakatos, Low-frequency neuronal oscillations as instruments of sensory selection. *Trends Neurosci.* **32**, 9–18 (2009).
3. P. Lakatos, G. Karmos, A. D. Mehta, I. Ulbert, C. E. Schroeder, Entrainment of neuronal oscillations as a mechanism of attentional selection. *Science* **320**, 110–113 (2008).
4. M. J. Henry, J. Obleser, Frequency modulation entrains slow neural oscillations and optimizes human listening behavior. *Proc. Natl. Acad. Sci. U.S.A.* **109**, 20095–20100 (2012).
5. M. R. Jones, H. Moynihan, N. MacKenzie, J. Puente, Temporal aspects of stimulus-driven attending in dynamic arrays. *Psychol. Sci.* **13**, 313–319 (2002).
6. A. Breska, L. Y. Deouell, Neural mechanisms of rhythm-based temporal prediction: Delta phase-locking reflects temporal predictability but not rhythmic entrainment. *PLOS Biol.* **15**, e2001665 (2017).
7. P. Praamstra, D. Kourtis, H. F. Kwok, R. Oostenveld, Neurophysiology of implicit timing in serial choice reaction-time performance. *J. Neurosci.* **26**, 5448–5455 (2006).
8. C. Minnissi, E. L. Wilding, J. T. Coull, A. C. Nobre, Orienting attention in time: Modulation of brain potentials. *Brain* **122**, 1507–1518 (1999).
9. J. T. Coull, A. C. Nobre, Where and when to pay attention: The neural systems for directing attention to spatial locations and to time intervals as revealed by both PET and fMRI. *J. Neurosci.* **18**, 7426–7435 (1998).

10. Á. Correa, J. Lupiáñez, P. Tudela, The attentional mechanism of temporal orienting: Determinants and attributes. *Exp. Brain Res.* **169**, 58–68 (2006).
11. M. I. Leon, M. N. Shadlen, Representation of time by neurons in the posterior parietal cortex of the macaque. *Neuron* **38**, 317–327 (2003).
12. Y. Komura, R. Tamura, T. Uwano, H. Nishijo, K. Kaga, T. Ono, Retrospective and prospective coding for predicted reward in the sensory thalamus. *Nature* **412**, 546–549 (2001).
13. H. Niki, M. Watanabe, Prefrontal and cingulate unit activity during timing behavior in the monkey. *Brain Res.* **171**, 213–224 (1979).
14. S. Roux, M. Coulmance, A. Riehle, Context-related representation of timing processes in monkey motor cortex. *Eur. J. Neurosci.* **18**, 1011–1016 (2003).
15. S. G. Heideman, F. van Ede, A. C. Nobre, Temporal alignment of anticipatory motor cortical beta lateralisation in hidden visual-motor sequences. *Eur. J. Neurosci.* **48**, 2684–2695 (2018).
16. S. G. Heideman, G. Rohenkohl, J. J. Chauvin, C. E. Palmer, F. van Ede, A. C. Nobre, Anticipatory neural dynamics of spatial-temporal orienting of attention in younger and older adults. *Neuroimage* **178**, 46–56 (2018).
17. A. Breska, L. Y. Deouell, When synchronizing to rhythms is not a good thing: Modulations of preparatory and post-target neural activity when shifting attention away from on-beat times of a distracting rhythm. *J. Neurosci.* **36**, 7154–7166 (2016).
18. M. Alegre, I. G. Gurtubay, A. Labarga, J. Iriarte, A. Malanda, J. Artieda, Alpha and beta oscillatory changes during stimulus-induced movement paradigms: Effect of stimulus predictability. *Neuroreport* **14**, 381–385 (2003).
19. M. A. Sherman, S. Lee, R. Law, S. Haegens, C. A. Thorn, M. S. Härmäläinen, C. I. Moore, S. R. Jones, Neural mechanisms of transient neocortical beta rhythms: Converging evidence from humans, computational modeling, monkeys, and mice. *Proc. Natl. Acad. Sci. U.S.A.* **113**, E4885–E4894 (2016).
20. R. Bartolo, L. Prado, H. Merchant, Information processing in the primate basal ganglia during sensory-guided and internally driven rhythmic tapping. *J. Neurosci.* **34**, 3910–3923 (2014).
21. G. Stefanics, B. Hangya, I. Hernadi, I. Winkler, P. Lakatos, I. Ulbert, Phase entrainment of human delta oscillations can mediate the effects of expectation on reaction speed. *J. Neurosci.* **30**, 13578–13585 (2010).
22. S. K. Herbst, J. Obleser, Implicit variations of temporal predictability: Shaping the neural oscillatory and behavioural response. *Neuropsychologia* **101**, 141–152 (2017).
23. D. Bolger, J. T. Coull, D. Schön, Metrical rhythm implicitly orients attention in time as indexed by improved target detection and left inferior parietal activation. *J. Cogn. Neurosci.* **26**, 593–605 (2014).
24. J. T. Coull, J. Cotti, F. Vidal, Differential roles for parietal and frontal cortices in fixed versus evolving temporal expectations: Dissociating prior from posterior temporal probabilities with fMRI. *Neuroimage* **141**, 40–51 (2016).
25. J. T. Coull, C. D. Frith, C. Büchel, A. C. Nobre, Orienting attention in time: Behavioural and neuroanatomical distinction between exogenous and endogenous shifts. *Neuropsychologia* **38**, 808–819 (2000).
26. J. A. Grahn, J. B. Rowe, Finding and feeling the musical beat: Striatal dissociations between detection and prediction of regularity. *Cereb. Cortex* **23**, 913–921 (2013).
27. J. T. Coull, A. C. Nobre, Dissociating explicit timing from temporal expectation with fMRI. *Curr. Opin. Neurobiol.* **18**, 137–144 (2008).
28. A. Breska, R. B. Ivry, Double dissociation of single-interval and rhythmic temporal prediction in cerebellar degeneration and Parkinson's disease. *Proc. Natl. Acad. Sci. U.S.A.*, 20180596 (2018).
29. M. Grube, F. E. Cooper, P. F. Chinnery, T. D. Griffiths, Dissociation of duration-based and beat-based auditory timing in cerebellar degeneration. *Proc. Natl. Acad. Sci.* **107**, 11597–11601 (2010).
30. S. Teki, M. Grube, S. Kumar, T. D. Griffiths, Distinct neural substrates of duration-based and beat-based auditory timing. *J. Neurosci.* **31**, 3805–3812 (2011).
31. M. Grube, K. H. Lee, T. D. Griffiths, A. T. Barker, P. W. Woodruff, Transcranial magnetic theta-burst stimulation of the human cerebellum distinguishes absolute, duration-based from relative, beat-based perception of subsecond time intervals. *Front. Psychol.* **1**, 171 (2010).
32. R. B. Ivry, S. W. Keele, Timing functions of the cerebellum. *J. Cogn. Neurosci.* **1**, 136–152 (1989).
33. R. M. C. Spencer, H. N. Zelaznik, J. Diedrichsen, R. B. Ivry, Disrupted timing of discontinuous but not continuous movements by cerebellar lesions. *Science* **300**, 1437–1439 (2003).
34. R. M. C. Spencer, T. Verstynen, M. Brett, R. B. Ivry, Cerebellar activation during discrete and not continuous timed movements: An fMRI study. *Neuroimage* **36**, 378–387 (2007).
35. R. Courtemanche, Y. Lamarre, Local field potential oscillations in primate cerebellar cortex: Synchronization with cerebral cortex during active and passive expectancy. *J. Neurophysiol.* **93**, 2039–2052 (2005).
36. T. D. Aumann, E. E. Fetz, Oscillatory activity in forelimb muscles of behaving monkeys evoked by microstimulation in the cerebellar nuclei. *Neurosci. Lett.* **361**, 106–110 (2004).
37. S. Ohmae, J. Kunimatsu, M. Tanaka, Cerebellar roles in self-timing for sub- and supra-second intervals. *J. Neurosci.* **37**, 3511–3522 (2017).
38. J. Kunimatsu, T. W. Suzuki, S. Ohmae, M. Tanaka, Different contributions of preparatory activity in the basal ganglia and cerebellum for self-timing. *eLife* **7**, e35676 (2018).
39. J. X. O'Reilly, M. M. Mesulam, A. C. Nobre, The cerebellum predicts the timing of perceptual events. *J. Neurosci.* **28**, 2252–2260 (2008).
40. K. Aso, T. Hanakawa, T. Aso, H. Fukuyama, Cerebro-cerebellar interactions underlying temporal information processing. *J. Cogn. Neurosci.* **22**, 2913–2925 (2010).
41. Y. Nagai, H. D. Critchley, E. Featherstone, P. B. C. Fenwick, M. R. Trimble, R. J. Dolan, Brain activity relating to the contingent negative variation: An fMRI investigation. *Neuroimage* **21**, 1232–1241 (2004).
42. J. Obleser, M. J. Henry, P. Lakatos, What do we talk about when we talk about rhythm? *PLOS Biol.* **15**, e2002794 (2017).
43. A. Breska, L. Y. Deouell, Dance to the rhythm, cautiously: Isolating unique indicators of oscillatory entrainment. *PLOS Biol.* **15**, e2003534 (2017).
44. J. M. Rimmelle, B. Morillon, D. Poeppel, L. H. Arnal, Proactive sensing of periodic and aperiodic auditory patterns. *Trends Cogn. Sci.* **22**, 870–882 (2018).
45. B. Zoefel, S. ten Oever, A. T. Sack, The involvement of endogenous neural oscillations in the processing of rhythmic input: More than a regular repetition of evoked neural responses. *Front. Neurosci.* **12**, 95 (2018).
46. S. Haegens, E. Zion Golumbic, Rhythmic facilitation of sensory processing: A critical review. *Neurosci. Biobehav. Rev.* **86**, 150–165 (2018).
47. C. Drake, M. C. Botte, Tempo sensitivity in auditory sequences: Evidence for a multiple-look model. *Percept. Psychophys.* **54**, 277–286 (1993).
48. E. Maris, R. Oostenveld, Nonparametric statistical testing of EEG- and MEG-data. *J. Neurosci. Methods* **164**, 177–190 (2007).
49. H. Merchant, W. Zarco, O. Perez, L. Prado, R. Bartolo, Measuring time with different neural chronometers during a synchronization-continuation task. *Proc. Natl. Acad. Sci.* **108**, 19784–19789 (2011).
50. M. J. Anderson, C. J. F. Ter Braak, Permutation tests for multi-factorial analysis of variance. *J. Stat. Comput. Simul.* **73**, 85–113 (2003).
51. J.-P. Lachaux, E. Rodriguez, J. Martinerie, F. J. Varela, Measuring phase synchrony in brain signals. *Hum. Brain Mapp.* **8**, 194–208 (1999).
52. R. Verleger, P. Japkowksi, E. Wascher, Evidence for an integrative role of P3b in linking reaction to perception. *J. Psychophysiol.* **20**, (2005).
53. E. Donchin, M. G. H. Coles, Is the P300 component a manifestation of context updating? *Behav. Brain Sci.* **11**, 357–374 (1988).
54. A. Correa, A. C. Nobre, Neural modulation by regularity and passage of time. *J. Neurophysiol.* **100**, 1649–1655 (2008).
55. S. A. Hillyard, Relationships between the contingent negative variation (CNV) and reaction time. *Physiol. Behav.* **4**, 351–357 (1969).
56. U. Boehm, L. van Maanen, B. Forstmann, H. van Rijn, Trial-by-trial fluctuations in CNV amplitude reflect anticipatory adjustment of response caution. *Neuroimage* **96**, 95–105 (2014).
57. B. Perfetti, C. Moisello, E. C. Landsness, S. Kvint, A. Pruski, M. Onofrij, G. Tononi, M. F. Ghilardi, Temporal evolution of oscillatory activity predicts performance in a choice-reaction time reaching task. *J. Neurophysiol.* **105**, 18–27 (2011).
58. C. M. Gómez, A. Delinte, E. Vaquero, M. J. Cardoso, M. Vázquez, M. Crommelinck, A. Roucoux, Current source density analysis of CNV during temporal gap paradigm. *Brain Topogr.* **13**, 149–159 (2001).
59. S. S. Dalal, D. Ospipa, O. Bertrand, K. Jerbi, Oscillatory activity of the human cerebellum: The intracranial electrocerebelogram revisited. *Neurosci. Biobehav. Rev.* **37**, 585–593 (2013).
60. F. Macar, F. Vidal, L. Casini, The supplementary motor area in motor and sensory timing: Evidence from slow brain potential changes. *Exp. Brain Res.* **125**, 271–280 (1999).
61. Á. Correa, J. Lupiáñez, E. Madrid, P. Tudela, Temporal attention enhances early visual processing: A review and new evidence from event-related potentials. *Brain Res.* **1076**, 116–128 (2006).
62. K. K. Ng, S. Tobin, T. B. Penney, Temporal accumulation and decision processes in the duration bisection task revealed by contingent negative variation. *Front. Integr. Neurosci.* **5**, 77 (2011).
63. H. van Rijn, T. W. Kononowicz, W. H. Meck, K. K. Ng, T. B. Penney, Contingent negative variation and its relation to time estimation: A theoretical evaluation. *Front. Integr. Neurosci.* **5**, 91 (2011).
64. A. Stancák, G. Pfürtscheller, Event-related desynchronization of central beta-rhythms during brisk and slow self-paced finger movements of dominant and nondominant hand. *Cogn. Brain Res.* **4**, 171–183 (1996).
65. H. Jasper, W. Penfield, Electrocorticograms in man: Effect of voluntary movement upon the electrical activity of the precentral gyrus. *Arch. Psychiatr. Nervenk.* **183**, 163–174 (1949).
66. N. Jenkinson, P. Brown, New insights into the relationship between dopamine, beta oscillations and motor function. *Trends Neurosci.* **34**, 611–618 (2011).

67. B. E. Kilavik, M. Zaepffel, A. Brovelli, W. A. MacKay, A. Riehle, The ups and downs of beta oscillations in sensorimotor cortex. *Exp. Neurol.* **245**, 15–26 (2013).
68. S. A. Kotz, A. Stockert, M. Schwartzze, Cerebellum, temporal predictability and the updating of a mental model. *Philos. Trans. R. Soc. B Biol. Sci.* **369**, 20130403 (2014).
69. S. Nozaradan, M. Schwartzze, C. Obermeier, S. A. Kotz, Specific contributions of basal ganglia and cerebellum to the neural tracking of rhythm. *Cortex* **95**, 156–168 (2017).
70. E. S. te Woerd, R. Oostenveld, F. P. de Lange, P. Praamstra, A shift from prospective to reactive modulation of beta-band oscillations in Parkinson's disease. *Neuroimage* **100**, 507–519 (2014).
71. P. Praamstra, P. Pope, Slow brain potential and oscillatory EEG manifestations of impaired temporal preparation in Parkinson's disease. *J. Neurophysiol.* **98**, 2848–2857 (2007).
72. E. S. te Woerd, R. Oostenveld, F. P. de Lange, P. Praamstra, Impaired auditory-to-motor entrainment in Parkinson's disease. *J. Neurophysiol.* **117**, 1853–1864 (2017).
73. R. F. Helfrich, A. Breska, R. T. Knight, Neural entrainment and network resonance in support of top-down guided attention. *Curr. Opin. Psychol.* **29**, 82–89 (2019).
74. P. Lakatos, G. Musacchia, M. N. O'Connal, A. Y. Falchier, D. C. Javitt, C. E. Schroeder, The spectrotemporal filter mechanism of auditory selective attention. *Neuron* **77**, 750–761 (2013).
75. E. Schröger, S. A. Kotz, F. Knolle, P. Baess, The cerebellum generates motor-to-auditory predictions: ERP lesion evidence. *J. Cogn. Neurosci.* **24**, 698–706 (2012).
76. M. Schwartzze, S. A. Kotz, A dual-pathway neural architecture for specific temporal prediction. *Neurosci. Biobehav. Rev.* **37**, 2587–2596 (2013).
77. R. B. Ivry, R. M. C. Spencer, H. N. Zelaznik, J. Diedrichsen, The cerebellum and event timing. *Ann. N. Y. Acad. Sci.* **978**, 302–317 (2002).
78. J. A. Grahn, M. Brett, Impairment of beat-based rhythm discrimination in Parkinson's disease. *Cortex* **45**, 54–61 (2009).
79. A. Breska, R. B. Ivry, Taxonomies of timing: Where does the cerebellum fit in? *Curr. Opin. Behav. Sci.* **8**, 282–288 (2016).
80. J. J. Paton, D. V. Buonomano, The neural basis of timing: Distributed mechanisms for diverse functions. *Neuron* **98**, 687–705 (2018).
81. J. L. Raymond, S. G. Lisberger, M. D. Mauk, The cerebellum: A neuronal learning machine? *Science* **272**, 1126–1131 (1996).
82. T. Schmitz-Hübsch, S. T. Du Montcel, L. Baliko, J. Berciano, S. Boesch, C. Depondt, P. Giunti, C. Globas, J. Infante, J. S. Kang, B. Kremer, C. Mariotti, B. Melega, M. Pandolfo, M. Rakowicz, P. Ribai, R. Rola, L. Schöls, S. Szymanski, B. P. Van De Warrenburg, A. Dürr, T. Klockgether, R. Fancello, Scale for the assessment and rating of ataxia: Development of a new clinical scale. *Neurology* **66**, 1717–1720 (2006).
83. D. H. Brainard, The psychophysics toolbox. *Spat. Vis.* **10**, 433–436 (1997).
84. T.-P. Jung, S. Makeig, C. Humphries, T.-W. Lee, M. J. McKeown, V. Iragui, T. J. Sejnowski, Removing electroencephalographic artifacts by blind source separation. *Psychophysiology* **37**, 163–178 (2000).
85. B. Philipp, CircStat: A MATLAB toolbox for circular statistics. *J. Stat. Softw.* **31**, 1–21 (2009).
86. V. Yakovlev, S. Fusi, W. Senn, Climbing neuronal activity as an event-based cortical representation of time. *J. Neurosci.* **24**, 3295–3303 (2004).
87. D. Durstewitz, Self-organizing neural integrator predicts interval times through climbing activity. *J. Neurosci.* **23**, 5342–5353 (2003).
88. J. Miller, T. U. I. Patterson, R. Ulrich, Jackknife-based method for measuring LRP onset latency differences. *Psychophysiology* **35**, 99–115 (1998).

Acknowledgments: We thank K. Duberg, C. Tischler, K. Andrade, and A. Saxena for assistance in collecting the data. **Funding:** This work was supported by grants from the National Institutes of Health (NIH) (NS092079 and NS105839). This research was supported by funding from the NIH (R35 NS116883). **Author contributions:** A.B. and R.B.I. conceived the study, designed the experiments, and wrote the paper. A.B. provided software, collected the data, and analyzed the data. **Competing interests:** The authors declare that they have no competing interests. **Data and materials availability:** All data needed to evaluate the conclusions in the paper are present in the paper and/or the Supplementary Materials. Additional data related to this paper may be requested from the corresponding author.

Submitted 31 January 2020

Accepted 15 October 2020

Published 2 December 2020

10.1126/sciadv.abb1141

Citation: A. Breska, R. B. Ivry, Context-specific control over the neural dynamics of temporal attention by the human cerebellum. *Sci. Adv.* **6**, eabb1141 (2020).

Science Advances

Context-specific control over the neural dynamics of temporal attention by the human cerebellum

Assaf Breska and Richard B. Ivry

Sci Adv **6** (49), eabb1141.
DOI: 10.1126/sciadv.eabb1141

ARTICLE TOOLS

<http://advances.sciencemag.org/content/6/49/eabb1141>

SUPPLEMENTARY MATERIALS

<http://advances.sciencemag.org/content/suppl/2020/11/30/6.49.eabb1141.DC1>

REFERENCES

This article cites 86 articles, 17 of which you can access for free
<http://advances.sciencemag.org/content/6/49/eabb1141#BIBL>

PERMISSIONS

<http://www.sciencemag.org/help/reprints-and-permissions>

Use of this article is subject to the [Terms of Service](#)

Science Advances (ISSN 2375-2548) is published by the American Association for the Advancement of Science, 1200 New York Avenue NW, Washington, DC 20005. The title *Science Advances* is a registered trademark of AAAS.

Copyright © 2020 The Authors, some rights reserved; exclusive licensee American Association for the Advancement of Science. No claim to original U.S. Government Works. Distributed under a Creative Commons Attribution NonCommercial License 4.0 (CC BY-NC).